Daniel Schaper [1], **Frank Meyer** [2]
[1] Institute of Communication Theory and Signal Processing,
[2] Laser Zentrum Hannover e.V.
[1] schaper@tnt.uni-hannover.de
[2] fm@lzh.de

OPTICAL SURFACE RECONSTRUCTION OF LASER STRUCTURED MICRO-OBJECTS

Abstract

A robust and process integrated quality control method for micro-technology components is a more and more important task in order to reduce production time and costs. This paper presents a measurement method easy integratable in laser systems, which are commonly used for manufacturing micro-technology components. Due to the limited space in the laser system, a passive optical depth from focus approach is chosen, in order to reconstruct a three-dimensional surface of the produced components.

keywords: *Process Integrated Quality Control, Depth from Focus, Laser System*

1 INTRODUCTION

Excimer lasers emitting pulsed UV radiation are widely used for micro-machining. The beam characteristic of such lasers with a top hat beam profile is well suited for mask imaging technology (fig. 1a). With this machining technology the laser beam is shaped by a mask and a reduced scale image in the micrometer range is projected on the surface of the sample by a lens. Due to the high fluence, and in case of polymers, photo chemical interactions of the machined material and the laser radiation, micro-ablation volumes can be removed. Complex structures are achieved by superpositioning of single ablation volumes. Therefore, a special numerical controlled (NC) machining process is employed. For the technical realization of the micro-machining with pulsed lasers, a variety of full automated precision machining centers have been developed to serve the high grade of laser manufacturing of micro-parts [1], [10]. An example of such a NC machining center developed at the Laser Zentrum Hannover e.V. is

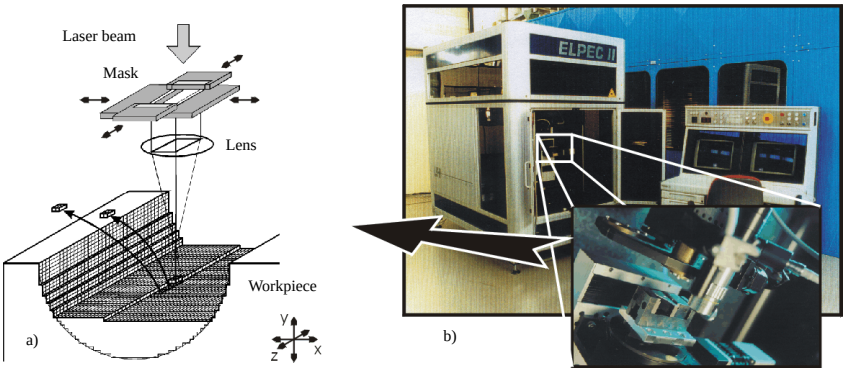

Fig. 1. a) Principle of 3D micro-machining by pulsed laser radiation. b) NC precision machining center ELPECmult. (Source: LZH)

shown in fig. 1b. Though, a wide number of materials can be structured with high accuracy on these machines, achieving an exact ablation depth is still problematic. One reason is that, due to the variety of parameters influencing the machining process (fluence, absorptance, actual temperature of the sample, etc.), a prediction of the exact ablation depth is difficult. Another reason is the fact, that a typical unevenness of the machined surface appears. This unevenness is a consequence of the given non-ideal cuboid shaped single ablation volumes, which cause ridges to appear between these ablations, as shown in fig. 2a. Both, the unpredictable ablation depth and the height of the ridges grow with the number of laser pulses treating the machined sample (fig. 2b). A variety of machining strategies have been worked out to reduce the described

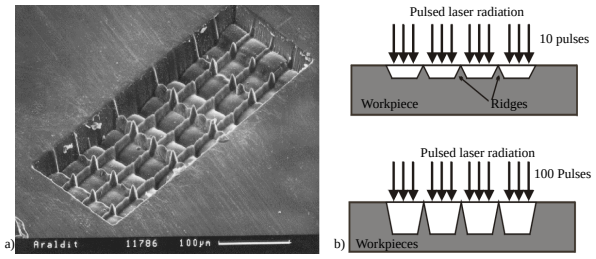

Fig. 2. a) SEM picture of a micro-cavity with ridges. b) Ridges growing by no. of laser pulses. (Source: LZH)

undesired geometric effects [9]. However, to decide on which strategy to use, it is important to have detailed information about the actual topography of the sample. To avoid the sample to be removed for external measurement, after which a repositioning is very delicate and time-consuming, systems for monitoring the unevenness of the structured workpiece surface are employed. These systems can be divided in non-optical and optical measurement principles. With non-optical systems like tactile sensors, the measurement of ditches in the micrometer range is problematic. Furthermore, the sensor touching the micro-structures surface causes

damage on sensitive materials. With an acoustic near field sensor this damage is prevented, but here, the necessary sensor-workpiece separation as small as 150 nm is inappropriate for machined samples with high aspects and scanning a 3-D surface of less than $1\ mm^2$ in high resolution may take several hours. Optical systems promise a more advanced monitoring and are therefore discussed in this proposal.

2 OPTICAL MEASUREMENT SYSTEMS

Optical measurement systems use a lens system for measuring and can be further subdivided into active and passive techniques. Active techniques are based on special reflective characteristics of the surface to be inspected. They use active illumination such as structured lighting, points, lines or harmonic lighting as used for Speckle interferometry. Photometric stereo uses different lighting directions in order to create a depth map. Passive techniques as stereo triangulation or focus / defocus based approaches instead can only inspect structured surfaces and use diffuse illumination. In order to develop an integrated measurement system a less complex passive system was chosen. Different passive approaches are discussed in the following paragraphs.

2.1 Stereo Image Analysis (SIA)

A depth map of an object is calculated based on two or even more images, taken from different cameras. Camera parameters and position of the cameras have to be calibrated. Depth is calculated via triangulation of the corresponding points in the two images. A common problem are outliers where no corresponding points can be found. As a result of the different camera views it may occur that some parts of the object are observed only in one image, known as ”occlusion”. Depth estimation is not possible in such cases [2]. Depth estimation can only be done for points lying in focus of the lens. Therefore SIA requires a detph of focus as large as possible. The used lens of the light microscope has a very small depth of focus. Finally, caused by the two cameras needed, an integration in the system would be more complicated than using a single camera as described below. Therefore the SIA approach is not suited for the target application.

2.2 Depth from Focus (DF)/ Depth from Defocus (DD)

With the Depth from Defocus method using only one camera, the depth estimation is done based on two images, one in focus and one in defocus with blurred areas [4]. With the grade of blur in the image taken, the depth map can be estimated. According to [2] depth maps obtained from DD are less precise than depth maps obtained from the DF approach. DF requires a couple of images with different known settings for e.g. lens position or focal length and searches the setting with best focus measure for each pixel. The depth map can be calculated from the chosen settings. Due to the small depth of focus of a light microscope the DF approach can be easily applied to the described application. An important advantage of the DF approach is the unexisting correspondence respectively occlusion problem known from SIA, and the microscope does not have to be calibrated. Therefore, the DF approach is chosen for monitoring objects after they have been processed by the laser.

3 SURFACE INSPECTION USING THE DEPTH FROM FOCUS TECHNIQUE

The DF technique exploits the fact that the distance between the camera and an object can be derived from a set of images taken at different camera parameter settings. Parameters which

can be varied are object distance g, focal distance of the used lens system f, apex angle of the lens system Θ (figure 3). Finding the parameter set for which an image point is nearest to the focal plane, leads to information about the relative depth as explained later. The circumstance allowing to detect the regions nearest to the focal plane can be shown at a wave-optics model. Assumed is an aberration free lens system with circular aperture and incoherent illumination. The projection is considered to be parallel due to the particular microscopes lens optic. Refraction index of the system is assumed to be $n = 1$. The system contains an entrance pupil respective an exit pupil summarised as E, causing the effect of aberrations. Figure 3 shows a spheric wave S_{o1} of object point O_1 and the corresponding spheric wave S_{i1} in image space and in focus point I_1. The spheric wave S_{o2} of a point O_2 causes the spheric wave S_{i2} in image space and an out of focus point I_2. The defect of focus distance w can also be specified by the optical distance Δz.

The mapping of a point of an object to the image can be explained by the Point Spread Function (PSF). The PSF in this case also known as Array Pattern [8] is described by:

$$h_f(r,\theta) = \frac{(\frac{2\pi}{\lambda}\sin\theta)^2}{\pi}\Big[\frac{J_1(\frac{2\pi}{\lambda}r\sin\theta)}{(\frac{2\pi}{\lambda}r\sin\theta)^2}\Big]^2 \tag{1}$$

Where J_1 is the Bessel function of first kind first order, λ the wave length of the used light and $\sin\theta$ the numerical aperture of the lens system. The Fourier transformation delivers the optical transfer function (OTF) of the system. It shows the lens system working as a filter. The OTF for a defocused system is described in [7]:

$$\begin{aligned} H_{df}(k) &= \frac{4}{\pi\alpha}\cos(\frac{1}{2}\alpha k)\Big\{\beta J_1(\alpha) + \sum_{n=1}^{\infty}(-1)^{n+1}\frac{\sin(2n\beta)}{2n} * [J_{2n-1}(\alpha) - J_{2n+1}(\alpha)]\Big\} \\ &\quad -\frac{4}{\pi\alpha}\sin(\frac{1}{2}\alpha k)\sum_{n=0}^{\infty}(-1)^{n}\frac{\sin(2n+1)\beta}{2n+1} * [J_{2n}(\alpha) - J_{2n+1}(\alpha)] \end{aligned} \tag{2}$$

wherein

$$\alpha = \frac{4\pi}{\lambda}wk \qquad \beta = cos^{-1}\frac{k}{2} \tag{3}$$

The defect of focus distance as mentioned before is described by w. Concerning [6] for small angles Θ and $\Delta z \ll i_1$ the relation between w and the distance from focal plane to defocused plane Δz can be described by:

$$w = \frac{1}{2}\Delta z \sin^2\Theta \tag{4}$$

Using Eq.(4) with Eq.(3) and Eq.(2) we get the OTF depending on spatial frequency k and the amount of defocus Δz. Figure 4 shows OTFs for different amounts of defocus. It can be seen that the more the amount of defocus Δz increases, the less higher frequencies are transfered. This circumstance allows to detect the image nearest to the focal plane. For this application a sequence of images was taken by varying the object to lens distance using a motorised micrometer lift table. If the projection is considered to be parallel, a change of the magnification can be neglected for a distance Δz between two observed levels. Several measures for the focus have been described. These are the amount of high frequencies, energy of image gradient, energy of image Laplacian [3] or the intensity of the image. For the application described in this paper the focus was measured by the variance within a window of size n*n. The value of focus is

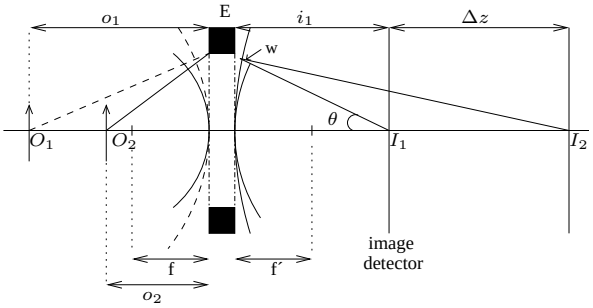

Fig. 3. Optics Model: spheric waves S_{o1},S_{02} caused by object points O_1,O_2 and corresponding spheric waves and points in image space. The defect of focus of point I_2 is described by w respectively the optical distance Δz.

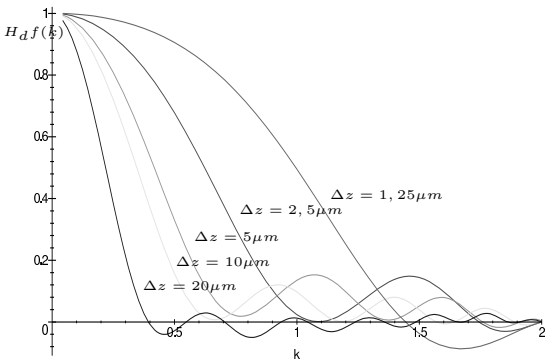

Fig. 4. Optical transfer function for the defocused system with different distances Δz from defocused plane to focal plane.

calculated for each pixel in each image of the image stack. Focus values of pixels located at the same position in an image are compared. The pixel nearest to the focal plane returns the maximum value. Figure 5 exemplarily shows three images of an image stack taken of a probe structured by an excimer laser. With information on the table position for the image containing the maximum value, the depth at this pixel position can be derived. The resolution in z-direction of the depth map depends on step size between two table positions Δz, characteristics of the lens and camera system. Lateral resolution depends on lens, respectively the numerical aperture of the system and wave length of the used light (concerning to Raleigh) and in this case on the window size chosen to calculate the local variances. In order to increase the accuracy in z-direction an interpolation can be applied to find the position of the variance maximum over all images. Different approaches are described to approximate the devolution of the focus, e.g. a Gaussian normal function [5]. In this application the devolution is approximated by a polynomial of second order.

4 EXPERIMENTAL RESULT

Figure 6 shows one image of the taken image stack of a micro-cavity structured by an excimer laser using a rectangular mask geometry. In Figure 7 the shaded 3-D model is presented. The cavity is divided by ridges. In order to reduce the effect of the ridges a machining strategy of overlapping related laser pulses has been used. This strategy results in two parallel ridges between neighbouring ablations in the model. The size of a single ablation is about $80\mu m * 80\mu m$. The depth of the hole is about 40 μm. For modelling the probe 20 images were taken and the distance Δ z was about 2.5 μm. The standard deviation derived for a known planar object using a step size of 2.5 μm was about 5 μm.

5 CONCLUSION

Integrated quality control of micro-technology components, structured with a laser system, using a DF approach delivers sufficiently accurate results in order to detect artefacts or ridges. The DF approach is a simple and stable method and is therefore usable in a real processing environment. The mechanism can be easily integrated in a commercial laser system. Due to

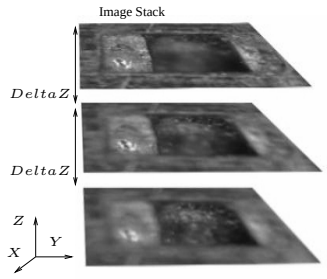

Fig. 5. Image Sequence with different object to sensor distance

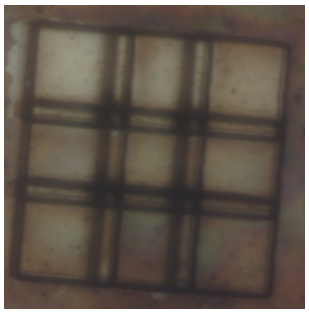

Fig. 6. Image of input data

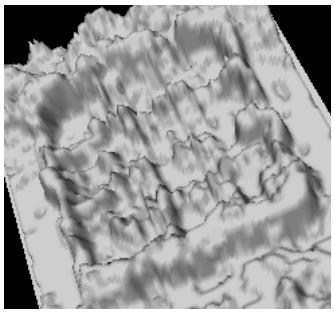

Fig. 7. Shaded 3-D model

an integration of a measurement technique in a laser system, the delicate and time consuming repositioning after external measurement is avoided.

REFERENCES

[1] A. Ostendorf et al., *Produktionsverfahren für die flexible Mikrostrukturierung passiver optischer Bauteile.*, Abschlussbericht FZKA-PFT 198, Laser Zentrum Hannover e.V., Projektträgerschaft Forschungszentrum Karlsruhe, 1999.

[2] M. Subbarao, G. Surya, *Depth from Defocus: A Spatial Domain Approach*, The Int. Jour. of Comp. Vision-13(3), pp 271-294, 1994.

[3] M. Noguchi, S.K. Nayar, *Microscopic Shape from Focus Using Active Illumination*, 12th IAPR Int. Conf. on Pattern Rec. Vol. 1, IEEE, pp 147-152, 1994.

[4] D. Ziou, *Passive Depth From Defocus Using a Spatial Domain Approach*, Tech. Report, DMI, Universite de Sherbrooke, Canada, 1997.

[5] A. Pentland, T. Darell, M. Turk, W. Huang, *A simple, real-time range camera*, IEEE, Conf. Comp. Vision a. Pattern Rec., pp256-261,1989.

[6] P. A. Stokseth, *Properties of a Defocused Optical System*, Jour. of Opt. Soc.of A., pp 1314-1321, 1969.

[7] H. H. Hopkins, *The concept of partial coherence in optics*, Proc. Roy. of London, pp 263, 1951.

[8] J. W. Goodmann, *Introduction to Fourier Optics*, Physical and Quantum Electronic Series, 1968.

[9] H. K. Tönshoff, F. von Alvensleben, A. Ostendorf,*Advanced Micro Machining with Excimer Lasers*, In: EUSPEN: Precision engineering nanotechnology, Bremen, 1999.

[10] H. K. Tönshoff, C. Graumann, M. Rinke, *Comparision of 3-D surfaces produced by 248 nm- and 193 nm-Excimer Laser Radiation*, SPIE‘s International Symposium on Intelligent Systems and Advanced Manufacturing, Boston, 1998.